Single Point Conducted EMI Sensor With Intelligent Inference for Detecting IT Appliances

Manoj Gulati, Shobha Sundar Ram, *Member, IEEE*, Angshul Majumdar, *Senior Member, IEEE*, and Amarjeet Singh, *Member, IEEE*

Abstract—Electrical grids need to embed smartness not just at the generation and distribution side but also at the consumption side. Specifically, in regard to office buildings, information technology (IT) loads such as desktops and printers, operating in non-working hours, can lead to significant energy wastage. Detailed understanding and quantification of this wastage can lead to motivational insights for reduction in this wastage. However, it is impractical to monitor such a large number of loads individually. In this paper, we propose a single point smart sensor to detect and track the operation of these IT appliances. Existing methods, based on state-of-the art sensors, have been ineffective at detecting IT loads that have time-varying power consumption patterns. Our proposed sensor detects IT loads using their common mode electromagnetic emissions (CM EMI) injected on the grid. The sensor is low cost, portable, and built using commercial off-the-shelf components. We use a nearest neighbor-based classification algorithm on the statistical features extracted from histograms of the measured CM EMI. Experimental evaluations carried out with multiple instances of commonly found IT appliances display up to 87% detection accuracy, thus validating the real world applicability of our proposed system.

Index Terms—Electromagnetic interference, smart sensors, buildings, appliance detection and classification.

I. INTRODUCTION

IN MANY developing countries, including India (the third largest consumer of electricity), the aggregate transmission and distribution losses (including theft) account for more than 50% of energy consumption [1]. Therefore, a unit of electricity saved at the consumption side is equal to two units produced. While there have been several research efforts over the last few years over developing smart grids on the transmission and distribution side [2]–[6], it is necessary to research techniques for incorporating smartness in the grids within the consumer premises [7]. On the consumption side, buildings, across the world, contribute to approximately 40% of the total energy expenditure. Offices, retail markets and educational institutes

absorb roughly 50% of this energy [8]. Within these buildings, heating, ventilation and air-conditioning (HVAC) are the dominant loads (40%), followed by information technology (IT) loads and lighting (25%) [9], [10]. While there has been considerable focus on optimizing the HVAC energy consumption, there is currently little work on energy optimization for IT loads [11], [12]. A significant portion of the IT load energy consumption arises from the wasteful operations of these loads during non-working hours [13]. The detection of these appliances can enable the quantification of energy wastage and this information, when provided as consumer feedback, can motivate energy conservation. In this work, we propose a low cost sensing solution that can be used to accurately detect the operation of these IT appliances within office spaces during off-hours. Let us first formulate the challenges that motivate and set apart this work:

1) Even a small office may have a large number of IT appliances. Therefore, the deployment and maintenance of an individual load monitor for each appliance, in a distributed setting, may quickly become prohibitive in terms of both cost and maintenance.

2) Single point sensing frameworks have been proposed (primarily for residential environments) for detecting appliances based on their energy usage patterns [14]–[23]. These include permanent loads that operate throughout the day (refrigerators and thermostats); on-off appliances (fans and lamps); loads based on finite-state machines (washing machines and dimmer lamps); and time-varying loads (IT loads). State of the art single point sensing solutions mainly involve exploiting information gathered from the power consumption characteristics for appliance detection [15]. Other works in the smart grid community proposed techniques to detect appliances using either physics based models derived from voltage and current waveforms [24] or from features extracted from the real and reactive power, wave shape and harmonic content [25]. As a result, while these solutions have been effective in detecting appliances of the first 3 categories, they have been unsuccessful in detecting IT appliances due to their time-varying power consumption pattern. Also, most of these techniques are limited by signal interference in the presence of multiple appliances. The problem is even more challenging in an office environment as the number of such appliances is large.

3) In much of the previous work on single point sensing for appliance detection, the proposed detection and classification systems were evaluated based on the test and the training data gathered from the same appliance. Such approaches assume that different instances of the same appliance (e.g., 2 different CFL lamps) will likely behave in the same manner. While this may be somewhat true at low sampling frequency, it must be experimentally validated at higher sampling frequencies as well. Accuracy of a single point sensing system should ideally be proved by training and testing on different appliance instances, for its general applicability in real world settings.

In this work, we develop a sensor for measuring high frequency common mode (CM) conducted electromagnetic interference (EMI) injected by the appliances on the power lines. The CM EMI is the common mode signal on both the phase and neutral lines with respect to the earth line. Since the EMI is a by-product of the power supply within the appliance, we hypothesize that the common mode EMI can be used to uniquely identify IT appliances such as laptops, CPUs and printers. Prior works have suggested using the differential EMI (DM EMI) between the phase and neutral lines for appliance detection [26]. However, DM EMI is an unreliable feature since the harmonics from the power supply and electrical infrastructure may interfere severely with the measurements [27]. Additionally, federal regulations mandate that all appliances are fitted with sophisticated filters for rejecting their DM emissions. Our second hypothesis is that we can use training data gathered from *one instance* of an appliance to classify *other instances* of the same make and model. Such a sensor offers an effective solution to detect IT appliances in office scenarios. This can eventually be used to identify their wasteful operations, thus contributing to the smartness on the consumption side in the grid.

Previously [26], [28]–[32] used bulky (and expensive) systems for EMI sensing such as Universal Software Radio Peripheral (USRP), vector network analyzers and spectrum analyzers. These systems cannot be easily modified to support CM measurements. Instead, we propose a low cost, portable, plug and play system for EMI sensing developed using commercial, off-the-shelf data acquisition systems. The classification algorithms, in prior works, were based on features extracted from frequency domain EMI data. They subsequently used a variety of algorithms such as k-nearest neighbor [26], neural networks [28] and support vector machines (SVM) [29] for classification. However, different appliances show considerable temporal variation in their EMI characteristics. To improve upon these results, we propose to employ statistics learnt from histograms of the EMI data. These histograms show consistency across time and across instances of the same type. While similar statistics have been previously used on time series data [33], this is the first time they are being used to discriminate electrical appliances based on their EMI signatures.

To summarize, the primary contributions of this work include: use of CM EMI as a feature for detection of time-varying IT loads; plug and play sensor for measurements;

classification protocol based on statistics extracted from histograms of measured CM EMI data; challenging test protocol, where different instances of appliances (of the same make and model) are used for training and testing thus bringing forth the challenges anticipated in real world settings. Our paper is organized as follows. In Section II, we discuss the background related to the use of CM EMI, its distinction from DM EMI, and its advantages for detecting IT loads. In Section III, we present a detailed description of the low-cost, portable sensor, made with COTS (commercial off-the-shelf) components, and associated signal-processing algorithms for classification of appliances. In Section IV, we present details of the experimental set up used to gather EMI data from 5 common office appliances namely CFL lamps, LCD monitors, CPUs, printers and laptops. We contrast the effectiveness of using histogram of the EMI data as an appliance signature instead of either the time-domain or frequency-domain data in Section V. We present the results from the nearest neighbor classification in Section VI. Similar classification process is followed for DM EMI data as well. Our results show a classification accuracy of 86.7% with CM EMI data compared to 45% with DM EMI data.

II. DESCRIPTION OF COMMON MODE AND DIFFERENTIAL MODE EMI

Most consumer and power appliances with switched mode power supplies (SMPS) inject EMI into the power lines as shown in Fig. 1. A single-phase power supply (or a single branch of a three phase power supply) consists of three power lines: the phase, neutral and earth, which are characterized by transmission line impedances Z. The power supply may be single ended (Fig. 1a) or split phase (Fig. 1b) with a 230V, 50Hz (Indian standard) between phase and neutral. In our work, we consider the more commonly found single ended supply where the neutral and earth terminals are shorted at the distribution transformer outlet. However, the principles we have outlined in this work are equally applicable to split phase power supplies. Electrical appliances are either three pin appliances (Fig. 1a) with earth connections or two pin appliances without an earth connection (Fig. 1b). EMI that is generated from the switching circuits in the appliance or due to the passives may be resolved into two components - (1) the differential mode (I_{dm}) component that is inserted into the power lines across the step down transformer that interfaces between the switching circuitry and the power lines and (2) the common mode (I_{cm}) component on both the phase and neutral, with respect to the local ground of the appliance. The CM noise is injected into the power lines through parasitic capacitances (C_T) in the transformer. Therefore, the current on the phase, neutral and earth lines are: $I_{cm}/2 + I_{dm}/2$, $I_{cm}/2 - I_{dm}/2$ and I_{cm} respectively. Note that the CM component exists even in single-phase supplies (Fig. 1a) due to the line impedances across the power lines. In the case of two pin appliances without an earth connection (not shown), the CM current loop is completed through a secondary coupling capacitance (C_P) between the phase and neutral terminals of the appliance and the local ground.
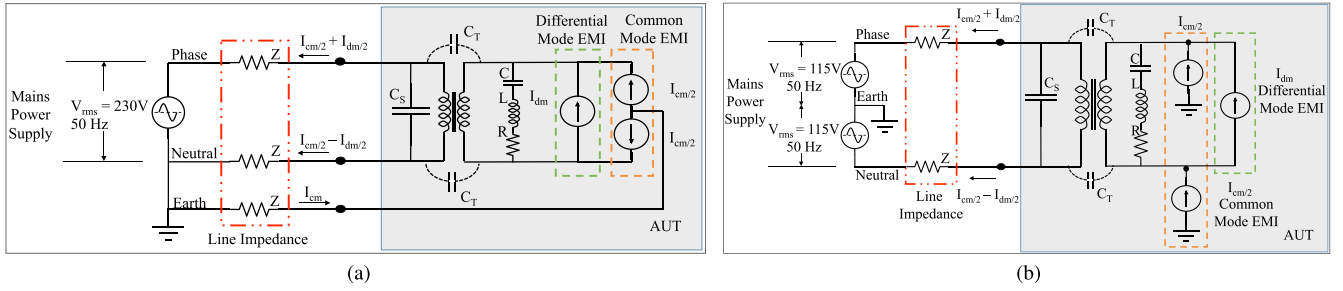
Fig. 1.   Equivalent circuit diagram of (a) single ended power supply connected to 3-pin appliance and of (b) split phase power supply connected to 2-pin appliance.

A. Comparison of DM and CM as Feature Vectors for Classification

Gupta *et al.* [26] postulated that appliances generate a unique and time-invariant DM EMI between the phase and neutral terminals, which can be exploited as a reliable feature vector for classification. However, [27] has shown several of the challenges associated with using the DM EMI as a reliable feature vector. First, DM noise currents, which are generated by inductive coupling through the transformer, mostly dominate high frequency bands. Therefore, these noise currents rapidly attenuate with increase in line impedance (or distance between the measurement outlet and the appliance outlet). In contrast, CM currents, which are generated at low frequencies due to capacitive coupling, are likely to attenuate more gradually with the increase in line impedance. Second, higher order harmonics of the power supply (230V, 50Hz) may dominate over the DM from appliances in many cases. In [26], they tackled this issue by carrying out background subtraction in the frequency domain in the logarithmic scale (or division in the linear scale). However, this results in the emergence of spurious artifacts in the frequency domain signatures of the appliances. In contrast, the earth wire (where the CM measurements can be made), is not meant for conduction of mains power supply and only meant for common mode leakage currents. As a result, the noise floor on CM measurements is likely to be much lower than DM. Third, there are federally mandated regulations on emission of DM noise from appliances so as to prevent the EMI from an appliance from interfering with the functioning of other appliances connected to the same grid. Therefore, most appliances come with inbuilt EMI filters that regulate the DM emission. In previous work [27], it was observed that the DM of some appliances such as laptops and CPUs was observed to be non-existent due to their EMI filters. The EMI filter of an appliance also significantly suppressed the DM of neighboring appliances on the power lines by offering their DM currents a low impedance path to ground. Therefore, appliances that may be detected independently may not be detected when they are powered simultaneously on the same lines. This may considerably reduce the efficacy of DM as a feature vector for detecting multiple appliances. In contrast, most appliances are not fitted with CM filters since CM noise is far less likely to impact the functioning of neighboring appliances. Despite this, if these appliances are fitted with CM filters, the electromagnetic behavior due to CM do not

significantly couple together. A detailed study of the CM and DM coupling between multiple appliances on a single power line is presented in Appendix A.

B. Measurement of CM and DM Components

In the case of split phase power supplies, the CM and DM can be measured by the sum and difference of phase (V_p) and neutral (V_n) voltages with respect to the earth measured at the power supply.

$$V_{CM} = V_p + V_n \qquad (1)$$
$$V_{DM} = V_p - V_n \qquad (2)$$

In single-phase power supplies, DM can be measured by the potential difference between the phase and the neutral. But the measurement of CM is more challenging. One method is to measure V_{dm} and V_p independently and estimate V_{cm} by subtracting V_{dm} from V_p. The advantage of this technique is that it can be applied to both two pin and three pin appliances. However, in practice, the performance of this technique is poor due to (1) the phase mismatch between DM and CM components and (2) because the magnitude of DM measurements usually exceeds the magnitude of CM by a few orders due to power supply harmonics. A second method is to directly measure the earth currents, which correspond to the CM components. The main advantage of this method is that the background noise across the earth lines is much lower than the phase and neutral lines. However, this technique can only be applied to three pin appliances due to the absence of a physical earth line connection in two pin appliances. The earth currents can be measured using either a current sense coil (such as the wide-band Rogowski coil) or through a current sense resistor. We have chosen to measure the current through the current sense resistor, to facilitate the development of a cheap sensor.

III. PROPOSED WORK

A. Plug and Play EMI Sensor Using Conducted EMI for Appliance Detection

In previous studies on EMI for non-intrusive load monitoring, measurements were made with spectrum analyzers and USRP boards [26], [28], [30]. These equipment are expensive and bulky. Hence, the measurements were mostly restricted to
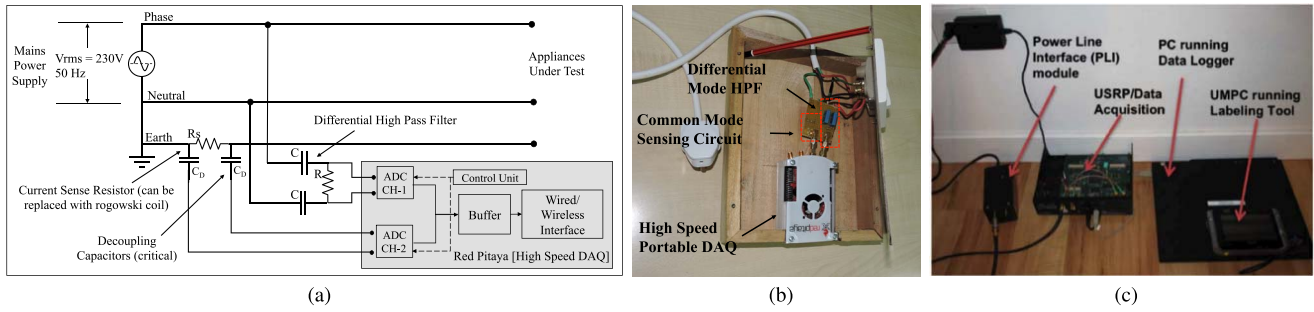
Fig. 2. Proposed EMI Sensor which is capable of simultaneously sensing CM and DM EMI on the mains power lines; (b) Actual prototype; (c) Reference viewgraph of the DM EMI sensor developed previously by [26]. The power line interface in (c) corresponds to the high pass filter in (b) and the USRP in (c) corresponds to the DAQ in (b).

laboratory conditions. On the other hand, electronic manufacturers measure the DM and CM emitted by appliances with expensive line impedance stabilization networks [34]. For the first time, we propose a low cost, portable sensor, made with off-the-shelf components, that is capable of simultaneously measuring both the CM and DM EMI components from appliances on the single phase (single ended) power lines. The DM component is estimated from the potential difference between the phase and neutral lines as shown in Fig. 2a. The power signal (230V, 50Hz) and some of its lower harmonics are removed from the signal through a differential high pass filter with a cut off frequency of 9kHz. The CM signal is estimated by measuring the voltage across a current sense resistor (R_s) on the earth line. Note that while the current sense resistor offers a cheap technique for measuring the CM currents, the deployment introduces a break in the connection between the power supply and the appliance (or the power line feeding multiple appliances). A non-intrusive, but more expensive alternative, would be to introduce a current sensing coil around the earth line. The data acquisition is carried out with the open source high speed Red Pitaya[1] board. The choice of the value of the current sense resistor is based on the ADC resolution and the shunt resistance shown in Fig. 3. The common mode voltage measured by the ADC is

$$V_{cm} = \frac{I_{cm}R_{shunt}R_s}{R_{shunt} + R_s} \qquad (3)$$

A low value of R_s (much lower than R_{shunt}) should be chosen to ensure minimum noise injection, while ensuring that the measured voltage is greater than V_{min}.

$$V_{cm} \approx I_{cm}R_s > V_{min} \qquad (4)$$

Here, V_{min} is the minimum voltage measurable with the ADC. In our case, the board is configured with a shunt resistance of 1MΩ and 16-bit ADC with 2V peak to peak (∴ $V_{min} = 0.131mV$). An empirically chosen value of 100Ω satisfied both the conditions and hence was found suitable for the current sense measurements.

Please note that placement of a current sense resistor in the earth line can pose a potential risk. Firstly, it can provide a path for high voltage (HV) signals to the DAQ. To avoid this safety hazard we have used two decoupling capacitors (C_D) as shown
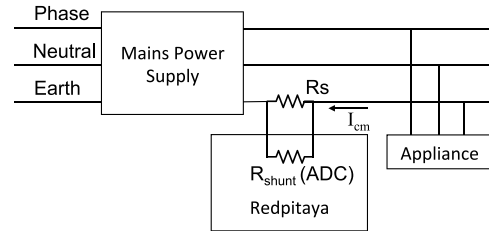
Fig. 3. Schematic showing connection diagram for current sense resistor (R_s) with shunt resistor R_{shunt} inside ADC on Red Pitaya.

in Fig. 2a to provide isolation from low-frequency (50Hz) HV signals. These capacitors (0.1uF each) are meant for HV operation, can operate at 480VAC and provide an isolation of 1.5kVDC (EPSON Part number B32023A3104M). Secondly, it violates the ground wire impedance regulations, which are 5Ω according to NFPA [35] and IEEE article number NEC 50.56 and 25Ω according to article number NEC 250.56 [36]. It can pose a risk to human using the appliance as 100Ω resistor grounds ground path for leakage currents. Currently, we are planning to tackle these issues in next non-intrusive version of this sensor.

Both the CM and DM data are acquired at a sampling frequency of 15.625MHz and stored in internal buffers. The data from the buffers can be loaded into a server or CPU for further processing through either an Ethernet or a wireless interface. This sensor can be easily modified to measure EMI from split phase power supplies. Instead, of directly measuring the DM and CM components, the phase (V_p) and neutral voltages (V_n) must be measured. The DM and CM components can be estimated through (1) and (2). There is, therefore, no requirement of a current sense resistor or coil in the case of split phase power supply measurements. The sensor can be directly plugged onto any electrical outlet of the building. The equivalent circuit of our proposed sensor is shown in Fig. 2a, Fig. 2b shows the actual prototype and Fig. 2c shows a contrasting sensing solution developed in [26]. All the stand-alone modules such as power line interface, data acquisition and data logging modules have been integrated into a single box in our proposed sensor.

B. Signal Processing and Feature Extraction

Consider that there are I appliance categories and J instances of each category. Accordingly, $x_{i,j}^s(t)$ represents
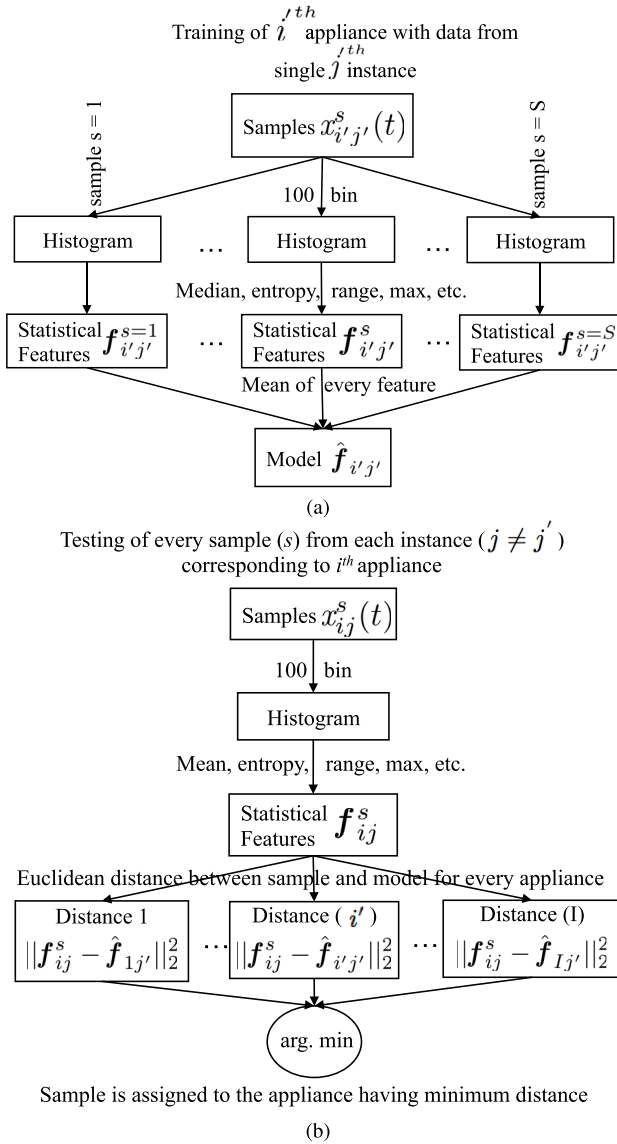
Fig. 4. Shows the flow chart with the steps followed during (a) training phase and (b) test phase.
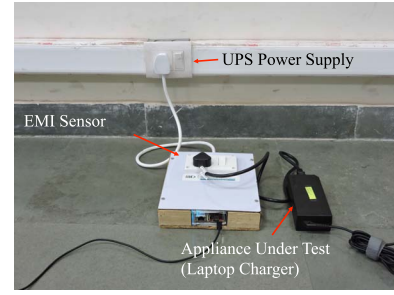

Fig. 5. Test setup shows the conducted EMI sensor used for common mode and differential mode EMI sensing for single ended power supply along with appliance under test.

multiple classes when we consider the magnitude of the measured data. Fig. 4a shows the pipeline followed during the training phase. The data from one instance (j'), of appliance category (i'), are used for training while the data from the remaining instances (test instances $j \neq j'$) are used for testing. The mean of the statistics, $\hat{f}_{i',j'}$ from all the traces corresponding to j', is used as the training model. Fig. 4b shows the test procedure. Each trace of the testing instances (j), corresponding to appliance category (i), is treated as a separate test case. A test case is classified based on the minimum Euclidean distance between the test vector, $f_{i,j}^s$, and the training models for all the appliances as shown below.

$$\underset{i'}{min} \left\| f_{i,j}^s - \hat{f}_{i',j'} \right\|_2^2 \vee i, j \neq j'. \tag{5}$$

IV. EXPERIMENTAL SETUP

The common IT loads and lighting sources in most offices are CPUs, LCD monitors, laptops, telephones, modems, wireless routers, printers and CFL lamps. Many published works on appliance detection note that several of these appliances, are very difficult to detect with single point sensing [17]–[19]. For instance, the time domain signatures of laptops and CPUs show considerable variation depending on the operational state of the appliance [37]. Hence, smart meters (with low sampling frequency) have not been successful in detecting these appliances. Additionally, these appliances are fitted with high quality EMI filters to reject DM EMI emission. Therefore, they are difficult to detect with DM EMI data. In this section, we show the utility of CM feature vector for successfully detecting some of these appliances. In most office setups, multiple appliances of the same type (make and model) are used due to logistical reasons. Due to practical considerations, only a single instance of an appliance can be used for generating training data for learning the features.

However, once the features are learnt, they must be useful for detecting other instances of the same appliance type. Therefore, in this work, our classification algorithm is trained on data from a single instance of each appliance category and is used to detect other instances of the same type. This test protocol marks a significant departure from previous works in this domain.

In this work, we surveyed the SMPS based electrical appliances in our institute, which includes faculty offices, research

a single trace or sample from S time-domain EMI traces measured for the jth instance of appliance category i. The time-domain data gathered by the sensor for each appliance are not directly used as a feature vector for classification because the measurements are not synchronized. Instead, we hypothesize that the CM EMI data from each appliance has a unique and time-invariant histogram that can be used as its signature. The histogram, derived from each sample (s), is obtained by binning the time domain data based on its magnitude. The distribution can be uniquely described by certain statistics. In this work, we extracted the following features from the histograms for classification: {entropy, skewness, interquartile range, kurtosis, percentile-75, range, maximum, median, percentile-90, mean absolute deviation}. The features are listed in the order of their effectiveness towards classification and form a vector for each sample trace ($f_{i,j}^s$). Features such as minimum and percentile-25 are not used since they look identical across

TABLE I
IT LOADS WITHIN THE INSTITUTE. HIGHLIGHTED APPLIANCES
WERE USED FOR THE EXPERIMENT

List of SMPS Appliances (connected to UPS)	Quantity	Power (Watts)	Total Power
Router	23	10	230
Projector	15	250	3750
Projector Screen Controller	5	10	50
CCTV Cameras	20	5	100
Fire Control Systems	2	250	500
Desktop (CPU + Monitors) HP LE1902x Hewlett Packard Compaq 8200 Tower	91	100	9100
RFID Access Control Systems	24	5	120
Laptop and Charger (Lenovo X1 20A80056I)	150	45	6750
A4 Sheet Scanner	10	25	250
Printer (HP LaserJet P1008)	55	700	38500
CFL(Crompton Greaves)	380	18	6840

labs, lecture halls and a small-scale data center. The complete list of appliances, their quantity, individual and aggregate power consumption are listed in Table I. Servers and air conditioners used in data center were not considered as part of this study, as they are already optimized for energy efficiency and hence scope for further improvement is minimal. In this survey, we found that CFLs, LCD monitors, CPUs, printers and laptops (highlighted in the table with their make and model details) were the most commonly used appliances accounting for over 92% of the energy consumption. Hence, we focused our study on the detection of these appliances.

We carried out the measurements inside the office precincts of our institute where the appliances are powered from an uninterrupted mains power supply (UPS). The EMI sensor, described in the previous Section, is connected to an outlet on an extension cord that is connected to the UPS. The appliance under test (AUT) was connected to the EMI sensor as shown in Fig. 5. We first examine the time-invariant characteristics of the CM-EMI signal. These results are presented in Appendix-B. Additional measurements are made on the power line without connecting any of the appliances. This is useful in determining the background noise on the power lines in the absence of the AUT. The EMI data collection from the twenty five individual appliances (five instances of each of the five appliance categories) spanned over a week from which we considered a data set spanning 5-6 hours (which includes measurement and logging time). This complete dataset[2] is released as part of this paper.

In the next two Sections, we discuss the measurement data and classification results for all appliances.

V. MEASUREMENT RESULTS

Time-domain CM and DM EMI are measured simultaneously for each individual instance of an appliance at a sampling frequency of 15.625MHz. Each time domain trace is 150ms long. A total of ten traces are collected for every appliance instance and there are 5 instances of each appliance. Corresponding amount of background data are also collected.

[2]https://goo.gl/wpxEh9

A. Frequency Domain Results

Fig. 6a and Fig. 6b show the frequency domain CM and DM signatures of an instance of each of the 5 appliances highlighted in Table I. The frequency range of interest is from DC to 5MHz. Before turning on the appliance, the background noise on the power lines are measured for each case. This exercise was carried out to monitor the change in the background noise characteristics in the power lines during the measurements. We note that across all the figures, the background noise in the CM measurements (-100dBm to -130dBm) is lower than the DM measurements (-60dBm to -120dBm). This is possibly because of the absence of power line harmonics and other fluctuations on the earth line where CM is measured. Secondly, we observe that above 4MHz, the frequency data look identical for all the appliances as it is dominated by the background noise on the power lines. Finally, the CM signatures are reasonably consistent across multiple instances of the same appliance make and model. This is not true for the case of DM. These results are not shown here due to constraints of space. In the case of the laptop charger (LC) and LCD monitor, a broad band CM noise can be discerned over the background noise floor, up to 2MHz. The average signal to noise ratio over this band of frequencies is 15dB and 20dB respectively. However, the poor DM to noise ratio, clearly shows that the EMI filters in the laptops and monitors have successfully removed all DM EMI. Therefore, the detection of these appliances is likely to be very poor if DM data are used as feature vectors for classification. Considerable CM and DM EMI are observed in the case of CFL. The average SNR across the entire frequency domain, are 30dB and 25dB respectively for CM and DM respectively. The EMI signatures from CFL are characterized by the fundamental peak, at 41.4kHz, corresponding to the switching frequency of the power supplies within the CFL and its higher order harmonics. Therefore, we anticipate that both CM and DM data can be successfully used for identifying CFLs. In the case of the CPU and printer, the background noise on the CM measurements were occasionally high. This may affect the classification results in these cases. In this work, we chose to not use the frequency domain data for machine learning and classification since a large portion of the data, from 4MHz to 7.8125MHz (half the sampling frequency) show significant overlap across the multiple appliances.

B. Histograms

Time domain measurements are not synchronized in any manner. Hence they show considerable variation across multiple instances of the same appliance and across time depending on the starting time (and phase) of the measurements. Therefore, these traces cannot be directly used as signatures for appliance classification. On the other hand, statistical distributions derived from the time domain data from the same appliance category may show similar features. We examine this by plotting the normalized number of counts per bin (histogram) of the magnitude of the CM EMI from each appliance category. Fig. 7 shows the histograms from two of the five appliance categories. Each of these histograms are drawn from data from a single time-domain trace of 150ms.
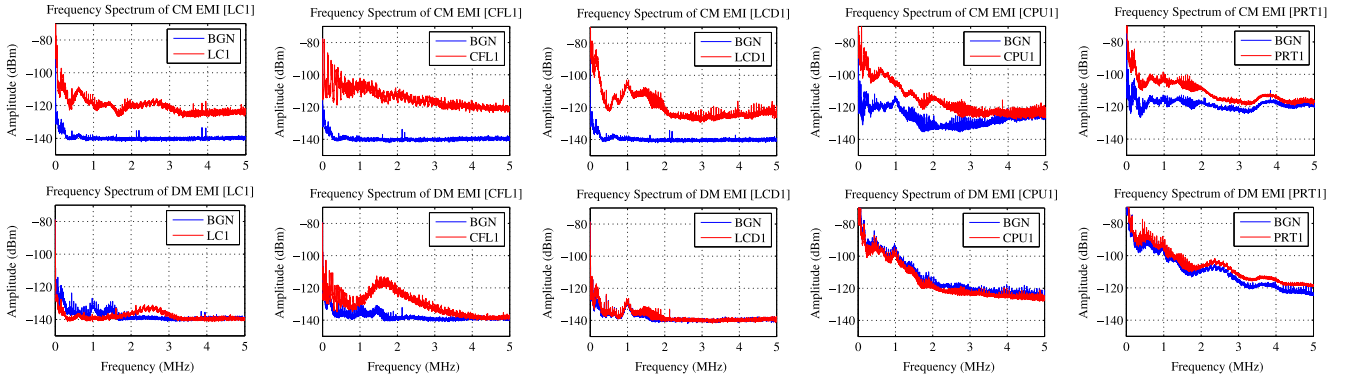
Fig. 6. Frequency domain plots showing (a) common mode EMI and (b) differential mode EMI measured from 5 appliances. They are Laptop charger (LC), CFL, LCD, CPU and Printer (PRT) (along with background noise (BGN) on the power lines before the appliance was turned on).
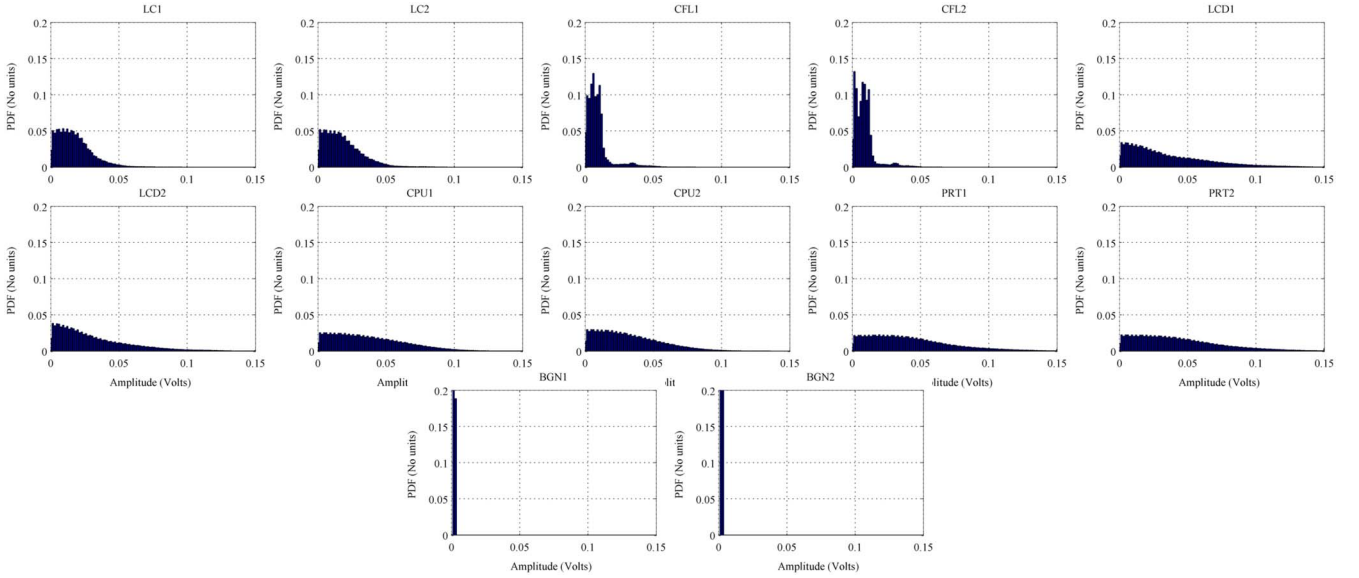

Fig. 7. Histogram (normalized number of counts per bin) of CM EMI data, of five appliances (from 2 of 5 instances) (a) Laptop charger (LC) (b) CFL (c) LCD (d) CPU (e) Printer (PRT) (f) Background noise (BGN) (when none of the appliances were operational), showing significant similarity across instances from same class of appliances.

The figures show the following features: the histograms of the measured voltages show considerable variation across different appliance categories. The most distinct histogram belongs to the CFL and the background noise category. On the other hand, the histograms show much smaller variation across multiple instances of the same appliance category. CPU, printer and LCD have roughly similar histograms. However, due to distinct peak values and width of slope in histograms, statistics such as kurtosis and skewness are able to capture this dissimilarity. Therefore, statistics (listed in Section III-B) that describe the histogram can form the basis for appliance detection and classification. DM data that are dominated by background noise show very similar histograms across multiple appliance categories. These histograms are not shown here due to constraints in space.

VI. CLASSIFICATION RESULTS AND DISCUSSION

As mentioned earlier, there are 6 categories in the classification - {*LCD monitor, Laptop Charger (LC), CFL, CPU,*

Printer (PRT) and Background (BGN)}. The last category, {*BGN*}, implies the absence of any of the other five IT appliances on the power line. 10 samples were measured for each of the 5 instances of every appliance category. Thus, I = 6, J = 5 and S = 10 based on the definitions provided in Section III-B.

The training model is the vector formed from the mean of the statistics drawn from the histograms corresponding to the samples of the training instance (20% of measured data). Each of the samples from the remaining four test instances form an individual test case (80% of measured data). Five-fold cross validation is carried out where the training and testing instances are swapped. As a result, there are a total of 200 (4 x 10 x 5) test samples corresponding to each appliance category. Each test case is assigned to one of the 6 appliance categories on the basis of the *minimum Euclidean distance* between the test feature vector and the training models as described in (5). We carry out the classification process using CM EMI data and then repeat the process with DM EMI data. We present the appliance confusion

matrix[3] along with precision and recall results from the nearest neighbor based classification algorithm on a per appliance basis in Table II(A) and Table II(B). The column headers, in the tables, indicate the classification classes whereas the row headers indicate the test classes. The highlighted features in the table indicate correctly identified test cases. The precision of appliance detection is computed as the ratio of correctly classified test cases of each appliance class (i) to the total number of traces classified as that appliance class. The total number, therefore, includes test traces from other appliances that are falsely classified to this particular class. The recall of an appliance, on the other hand, is computed as the number of correctly classified test cases of each appliance class to the total number of traces from that appliance class. Therefore, some of the traces of this class have been missed (or falsely identified as belonging to another class).

$$precision|_i = \frac{correct\ class|_i \times 100}{correct\ class|_i + false\ class|_i} \quad (6)$$

$$recall|_i = \frac{correct\ class|_i \times 100}{correct\ class|_i + missed\ class|_i} \quad (7)$$

Together, the precision and recall indicate the accuracy of the classification algorithm and the efficacy of the chosen feature vector. The following inferences can be drawn from the results: the average CM EMI precision and recall results (87.3% and 86.8% respectively) are far superior to the DM EMI precision and recall results (49.6%, 45.2% respectively). This validates the key hypothesis of our paper that CM EMI is a far superior feature for IT appliance detection compared to DM EMI. The poor performance of the DM results can be attributed to the high background noise (-60 to -120dBm) that dominated the DM measurements as seen in Fig. 6b. The *background* results in the CM EMI case is 100% (both precision and recall) compared to the low values for DM EMI. This is because of the distinct low noise floor that was observed in the CM EMI measurements due to the absence of the power signal and its higher order harmonics.

Past research efforts, using either smart meters or DM EMI, have reported the challenges in detecting IT appliances such as laptop chargers, LCD monitors and printers [27], [37]. This is because these appliances show considerable variation in their smart meter readings while operating in different modes (standby, hibernation, full operation and so on) [37]. Since these appliances are usually fitted with powerful DM EMI filters, they show very poor performance with respect to DM EMI (16.5%, 33.5% and 39.5% recall for laptop chargers, LCD monitors and printers respectively). The high precision and low recall value for printers, in the DM EMI case, is due to the poor SNR in the measurements due to the high background noise values. The classification of printers is therefore, largely on the basis of background noise rather than EMI signal itself. Nevertheless, these appliances are accurately detected with their CM EMI signatures (above 90% precision and recall for laptop chargers and printers; 72% for LCD monitors). CFLs can be accurately detected using either DM EMI or CM EMI data due to their strong and unique signatures and the absence

[3]https://en.wikipedia.org/wiki/Confusion_matrix

TABLE II
RESULTS FROM NEAREST NEIGHBOR BASED CLASSIFICATION ON
(A) CM EMI DATA AND (B) DM EMI DATA ON 6 CLASSES
(5 APPLIANCES AND BACKGROUND): (A)

(A)

	BGN	LC	LCD	CFL	CPU	PRT	Recall (%)
BGN	200	0	0	0	0	0	100
LC	0	197	3	0	0	0	98.5
LCD	0	15	144	0	33	8	72
CFL	0	0	0	200	0	0	100
CPU	0	0	12	0	119	69	59.5
PRT	0	0	1	0	17	182	91
Precision (%)	100	92.9	90	100	70.4	70.3	

(B)

	BGN	LC	LCD	CFL	CPU	PRT	Recall (%)
BGN	99	30	61	0	10	0	49.5
LC	106	33	43	0	18	0	16.5
LCD	87	29	67	0	17	0	33.5
CFL	3	4	0	193	0	0	96.5
CPU	51	22	38	0	69	20	34.5
PRT	7	5	12	0	97	79	39.5
Precision (%)	28.1	26.8	30.3	100	32.7	79.6	

of any type of EMI filters (DM and CM). Desktop CPUs show some improvement from DM EMI to CM EMI (from 35% to 60%). However, these appliances still remain challenging to detect. This can be attributed to the high background noise floor in the CM measurements of the CPUs (refer Fig. 6).

In this work (and all other prior works related to EMI sensing), the feature extraction for classification is carried out when the appliances are individually connected to the power lines. We have limited the study to one appliance at a time in order to evaluate the signal quality, stability and consistency across multiple instances of same appliance. In order to detect an appliance in the presence of multiple appliances on the grid, more complex appliance features (as opposed to the simple statistical features used in this work), extracted from dictionary-learning techniques may be needed. However, CM EMI will still serve as a useful signal for classification since CM EMI (unlike DM EMI) does not couple between multiple appliances. Therefore, this problem presents a unique opportunity for future research in this field. Secondly, while the sensing solution presented in this work detects and classifies appliances on the power lines, the technique does not provide information regarding the actual energy dissipation by the appliance. The second piece of information can, however, be gathered by operating a simple energy meter in conjunction with the proposed EMI sensor.

VII. CONCLUSION

IT loads such as LCD monitors, laptops and desktop CPUs constitute a significant proportion of energy wastage in office spaces when they are left operational during non-working hours. Current single point sensing solutions with smart energy meters have been unsuccessful in detecting these loads, due to their dynamic power consumption patterns. All of these appliances (and many more) generate CM EMI on the phase and

neutral power lines with respect to the earth at low frequencies through capacitive coupling as well as DM EMI between the phase and neutral at higher frequencies through inductive coupling. The DM EMI is difficult to detect due to the presence of EMI filters on the appliances as well as harmonics of the mains power supply. The CM EMI, on the other hand, has a much higher signal to noise ratio.

A significant advancement is made in this research in terms of the systems used for measuring EMI. Until now, bulky and expensive equipment constitute system setup for EMI measurements. In this work, both CM and DM EMI were measured simultaneously with a small and portable sensor made of commercial, off-the-shelf components. In the case of single ended power supplies, the CM EMI is estimated by measuring the earth currents. This measurement method is, however, limited to three pin appliances and not two-pin appliances. In split phase power supplies, the CM EMI can be measured by the mean of the phase and neutral voltages with respect to the earth.

Our experiments show that the histograms of CM EMI measured from IT appliances are reasonably time-invariant and consistent across multiple instances of appliances of the same make and model. Signature feature vectors of 5 IT appliances and the background electrical infrastructure are learnt from statistics extracted from their histograms. These training models are formed from data collected from a single instance of the appliance and used to classify other instances of the same make and model. This is a rather challenging protocol that is important in office scenarios where there is a high likelihood of finding many appliances of the same make and model. We found that, CM EMI forms a better feature, than any other feature researched so far, for detecting many of the IT based appliances. Additionally, since the CM EMI signal arises from the switched mode power supplies within electrical appliances, the proposed method is not limited to IT appliances, and can be extended to other SMPS appliances in residential and office settings as well. Future directions to this work are to investigate the possibility of using these features for load disaggregation of appliances with dynamic power consumption, which is the holy grail of non-intrusive load monitoring.

APPENDIX A
CM EMI COUPLING BEHAVIOR ACROSS MULTIPLE APPLIANCES

In prior work, we studied how DM EMI coupled between neighboring appliances using simulation models of appliance SMPS [27]. Here, we analyze the CM EMI coupling between two appliances (AUT-1 and AUT-2) using a generalizable model shown in Fig. 8. Each appliance is fitted with a distinct CM and DM EMI source. First, we consider the case when neither of the appliances are fitted with filters (Fig. 8 without DM and CM filters).

Fig. 9a shows the corresponding CM and DM EMI spectrums. The spectrums shows superposition of signals from both the appliances - CM peaks at 100kHz (AUT-1) and 130kHz peaks (AUT-2) and DM peaks at 40kHz (AUT-1) and 50kHz peaks (AUT-2). Since the amplitudes of both the CM and
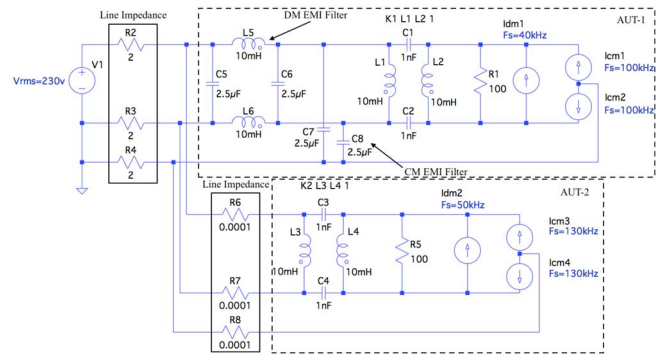

Fig. 8. A generalizable model for analyzing CM and DM EMI coupling mechanism between two appliances (AUT1 and AUT2), having DM and CM EMI filters.
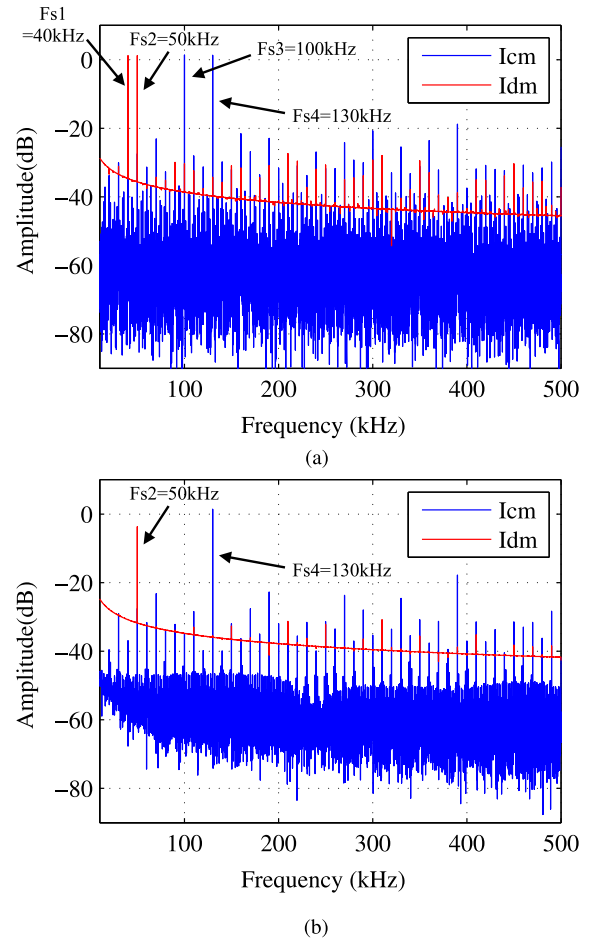

(a)

(b)

Fig. 9. CM and DM EMI spectrum showing coupling mechanism between two appliances (AUT1 and AUT2) (a) without any EMI filter and (b) with DM and CM EMI filter.

DM current sources are assumed to be 1A, the peaks of the corresponding signals in the EMI spectrums are of equal magnitude.

Next, we consider the case when a DM EMI and CM EMI filter are applied to AUT-1 [34], [38]. In an ideal scenario, these filters should only suppress the EMI from AUT-1 and have no impact on the neighboring AUT-2. The resulting spectrums, shown in Fig. 9b show that the DM EMI and CM EMI
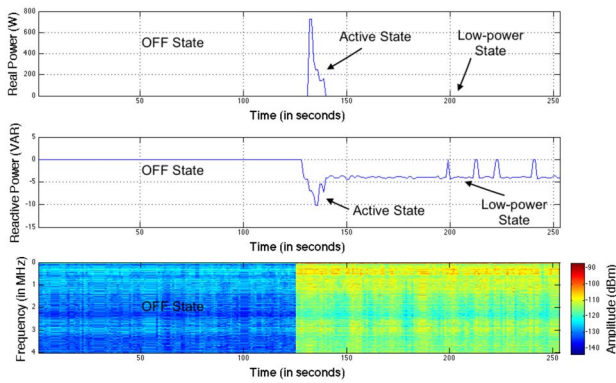
Fig. 10. Shows (a) real power (b) reactive power and (c) CM EMI spectrum measured from desktop printer in three different states (off, active and low power).
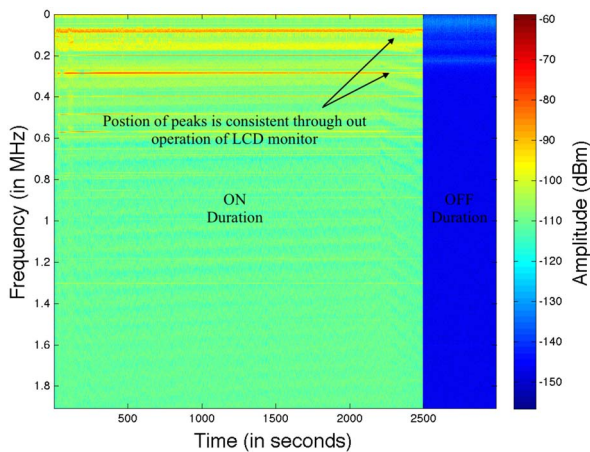

Fig. 11. Shows CM EMI spectrum measured from LCD monitor. This spectrum clearly shows consistent EMI peaks throughout operation of LCD monitor.

from AUT-1 are attenuated by approximately 40dB by their respective filters. Interestingly, the DM EMI from AUT-2 is also attenuated (by approximately 8dB) by the filter in AUT-1. This attenuation can severely impact the detection of DM EMI signals especially in low SNR scenarios as discussed in [26]. On the other hand, the CM EMI of AUT-2 is not affected by the filter in AUT-1. Therefore, this study suggests that CM EMI signals are less prone to interference between neighboring appliances and theoretically should still be detected.

APPENDIX B
TIME-INVARIANCE PROPERTY OF THE CM-EMI SIGNALS

In this section, we investigate the time-invariance nature of the CM EMI signals of simple commonly found IT appliances that have two operational states active and low power, besides the off state. Fig. 10 shows the CM EMI measured from a printer along with the corresponding real and reactive power measured by a smart meter. When the SMPS is powered off (off-state), we do not observe any EMI. However, the SMPS remains active with constant EMI in both the active state and low-power state even though the actual load differs. In the low

power state, there is non-zero reactive power consumption and no real power consumption while the active state has non-zero reactive and real power consumption.

Next, we considered an LCD monitor connected to a desktop CPU on which a variety of programs are run over a duration of an hour. Fig. 11 shows the corresponding CM EMI spectrum (up to 2MHz) measured from the monitor. The figure shows that despite the time-varying operations by the monitor, the EMI spectrum remains consistent.

The findings from this paper may not apply to multi-state domestic appliances that have closed loop controllers and show adaptive EMI behavior according to the instantaneous load condition [39].

REFERENCES

[1] S. Keshav and C. Rosenberg, "How Internet concepts and technologies can help green and smarten the electrical grid," *ACM SIGCOMM Comput. Commun. Rev.*, vol. 41, no. 1, pp. 109–114, 2011.
[2] A.-H. Mohsenian-Rad, V. W. S. Wong, J. Jatskevich, R. Schober, and A. Leon-Garcia, "Autonomous demand-side management based on game-theoretic energy consumption scheduling for the future smart grid," *IEEE Trans. Smart Grid*, vol. 1, no. 3, pp. 320–331, Dec. 2010.
[3] M. Pipattanasomporn, H. Feroze, and S. Rahman, "Multi-agent systems in a distributed smart grid: Design and implementation," in *Proc. IEEE/PES Power Syst. Conf. Expo. (PSCE)*, Seattle, WA, USA, 2009, pp. 1–8.
[4] J. Medina, N. Muller, and I. Roytelman, "Demand response and distribution grid operations: Opportunities and challenges," *IEEE Trans. Smart Grid*, vol. 1, no. 2, pp. 193–198, Sep. 2010.
[5] A. A. Aquino-Lugo, R. Klump, and T. J. Overbye, "A control framework for the smart grid for voltage support using agent-based technologies," *IEEE Trans. Smart Grid*, vol. 2, no. 1, pp. 173–180, Mar. 2011.
[6] F. Li *et al.*, "Smart transmission grid: Vision and framework," *IEEE Trans. Smart Grid*, vol. 1, no. 2, pp. 168–177, Sep. 2010.
[7] X. Fang, S. Misra, G. Xue, and D. Yang, "Smart grid—The new and improved power grid: A survey," *IEEE Commun. Surveys Tuts.*, vol. 14, no. 4, pp. 944–980, 4th Quart., 2012.
[8] B. Sisson and C. Van Aerschot, "Energy efficiency in buildings: Business realities and opportunities," World Bus. Council Sustain. Develop., Geneva, Switzerland, Tech. Rep., 2007.
[9] *Etechnology Roadmap Energy-Efficient Buildings: Heating and Cooling Equipment*, IEA, Singapore, 2011.
[10] L. Pérez-Lombard, J. Ortiz, and C. Pout, "A review on buildings energy consumption information," *Energy Build.*, vol. 40, no. 3, pp. 394–398, 2008.
[11] Y. Agarwal, B. Balaji, S. Dutta, R. K. Gupta, and T. Weng, "Dutycycling buildings aggressively: The next frontier in HVAC control," in *Proc. IEEE 10th Int. Conf. Inf. Process. Sensor Netw. (IPSN)*, Chicago, IL, USA, 2011, pp. 246–257.
[12] M. Jain, A. Singh, and V. Chandan, "Non-intrusive estimation and prediction of residential AC energy consumption," in *Proc. IEEE Int. Conf. Pervasive Comput. Commun. (PerCom)*, Sydney, NSW, Australia, 2016, pp. 1–9.
[13] O. T. Masoso and L. J. Grobler, "The dark side of occupants' behaviour on building energy use," *Energy Build.*, vol. 42, no. 2, pp. 173–177, 2010.
[14] G. W. Hart, "Nonintrusive appliance load monitoring," *Proc. IEEE*, vol. 80, no. 12, pp. 1870–1891, Dec. 1992.
[15] M. Zeifman, C. Akers, and K. Roth, "Nonintrusive appliance load monitoring (NIALM) for energy control in residential buildings: Review and outlook," *IEEE Trans. Consum. Electron.*, vol. 57, no. 1, pp. 76–84, Feb. 2011.
[16] J. M. Gillis, S. M. Alshareef, and W. G. Morsi, "Nonintrusive load monitoring using wavelet design and machine learning," *IEEE Trans. Smart Grid*, vol. 7, no. 1, pp. 320–328, Jan. 2016.

[17] M. Dong, P. C. M. Meira, W. Xu, and W. Freitas, "An event window based load monitoring technique for smart meters," *IEEE Trans. Smart Grid*, vol. 3, no. 2, pp. 787–796, Jun. 2012.

[18] D. He, W. Lin, N. Liu, R. G. Harley, and T. G. Habetler, "Incorporating non-intrusive load monitoring into building level demand response," *IEEE Trans. Smart Grid*, vol. 4, no. 4, pp. 1870–1877, Dec. 2013.

[19] Z. Wang and G. Zheng, "Residential appliances identification and monitoring by a nonintrusive method," *IEEE Trans. Smart Grid*, vol. 3, no. 1, pp. 80–92, Mar. 2012.

[20] J. Froehlich *et al.*, "Disaggregated end-use energy sensing for the smart grid," *IEEE Pervasive Comput.*, vol. 10, no. 1, pp. 28–39, Jan./Mar. 2011.

[21] N. Batra, M. Gulati, A. Singh, and M. B. Srivastava, "It's different: Insights into home energy consumption in India," in *Proc. 5th ACM Workshop Embedded Syst. Energy Efficient Build.*, Rome, Italy, 2013, pp. 1–8.

[22] N. Batra *et al.*, "NILMTK: An open source toolkit for non-intrusive load monitoring," in *Proc. 5th Int. Conf. Future Energy Syst.*, Cambridge, U.K., 2014, pp. 265–276.

[23] N. Batra, M. Gulati, P. Jain, K. Whitehouse, and A. Singh, "Bits and watts: Improving energy disaggregation performance using power line communication modems: Poster abstract," in *Proc. 1st ACM Conf. Embedded Syst. Energy Efficient Build.*, Memphis, TN, USA, 2014, pp. 210–211.

[24] D. He, L. Du, Y. Yang, R. Harley, and T. Habetler, "Front-end electronic circuit topology analysis for model-driven classification and monitoring of appliance loads in smart buildings," *IEEE Trans. Smart Grid*, vol. 3, no. 4, pp. 2286–2293, Dec. 2012.

[25] T. Hassan, F. Javed, and N. Arshad, "An empirical investigation of V–I trajectory based load signatures for non-intrusive load monitoring," *IEEE Trans. Smart Grid*, vol. 5, no. 2, pp. 870–878, Mar. 2014.

[26] S. Gupta, M. S. Reynolds, and S. N. Patel, "ElectriSense: Single-point sensing using EMI for electrical event detection and classification in the home," in *Proc. 12th ACM Int. Conf. Ubiquitous Comput.*, Copenhagen, Denmark, 2010, pp. 139–148.

[27] M. Gulati, S. S. Ram, and A. Singh, "An in depth study into using EMI signatures for appliance identification," in *Proc. 1st ACM Conf. Embedded Syst. Energy Efficient Build.*, Memphis, TN, USA, 2014, pp. 70–79.

[28] M. Enev, S. Gupta, T. Kohno, and S. N. Patel, "Televisions, video privacy, and powerline electromagnetic interference," in *Proc. 18th ACM Conf. Comput. Commun. Security*, Chicago, IL, USA, 2011, pp. 537–550.

[29] S. S. Clark *et al.*, "Current events: Identifying Webpages by tapping the electrical outlet," in *Proc. Eur. Symp. Res. Comput. Security*, Egham, U.K., 2013, pp. 700–717.

[30] K.-Y. Chen, G. A. Cohn, S. Gupta, and S. N. Patel, "uTouch: Sensing touch gestures on unmodified LCDs," in *Proc. SIGCHI Conf. Human Factors Comput. Syst.*, Paris, France, 2013, pp. 2581–2584.

[31] G. Cohn, D. Morris, S. N. Patel, and D. S. Tan, "Your noise is my command: Sensing gestures using the body as an antenna," in *Proc. SIGCHI Conf. Human Factors Comput. Syst.*, Vancouver, BC, Canada, 2011, pp. 791–800.

[32] M. Gulati, V. K. Singh, S. K. Agarwal, and V. A. Bohara, "Appliance activity recognition using radio frequency interference emissions," *IEEE Sensors J.*, vol. 16, no. 16, pp. 6197–6204, Aug. 2016.

[33] T. W. Anderson, *The Statistical Analysis of Time Series*, vol. 19. Hoboken, NJ, USA: Wiley, 2011.

[34] C. R. Paul, *Introduction to Electromagnetic Compatibility*, vol. 184. New York, NY, USA: Wiley, 2006.

[35] *Ground Impedance*, Fluke, Everett, WA, USA, 2016. [Online]. Available: https://support.fluke.com/find-sales/Download/Asset/2633834_6115_ENG_A_W.PDF

[36] (2016). *NEC*. [Online]. Available: http://fyi.uwex.edu/mrec/files/2011/04/W4.-Biesterveld-NEC-grounding-MREC2010.pdf

[37] S. Barker, S. Kalra, D. Irwin, and P. Shenoy, "Empirical characterization and modeling of electrical loads in smart homes," in *Proc. IEEE Int. Green Comput. Conf. (IGCC)*, Arlington, VA, USA, 2013, pp. 1–10.

[38] *All About EMI Filters*, TDK, Tokyo, Japan, 2016. [Online]. Available: http://us.tdk-lambda.com/ftp/other/all_about_emi_epmag.pdf

[39] K.-Y. Chen, S. Gupta, E. C. Larson, and S. Patel, "DOSE: Detecting user-driven operating states of electronic devices from a single sensing point," in *Proc. IEEE Int. Conf. Pervasive Comput. Commun. (PerCom)*, St. Louis, MO, USA, 2015, pp. 46–54.

Manoj Gulati received the B.Tech. degree in electronics engineering from Maharishi Dayanand University in 2011. He is currently pursuing the Ph.D. degree with the Indraprastha Institute of Information Technology, New Delhi. He was an Electronics Design Engineer with Hewlett Packard Educational Services, Noida, India, for two years, and Indrion Technologies, Bengaluru, India.

Shobha Sundar Ram received the B.Tech. degree in electronics and communication engineering from the University of Madras in 2004, and the M.S. and Ph.D. degrees in electrical engineering from the University of Texas at Austin, Austin, TX, USA, in 2006 and 2009, respectively. She was a Research and Development Electrical Engineer with Baker Hughes Inc., Houston, TX, USA, for three years. She joined the faculty of Indraprastha Institute of Information Technology, New Delhi, in 2013.

Angshul Majumdar received the B.Tech. degree in electrical engineering from Bengal Engineering and Science University in 2005, and the M.S. and Ph.D. degrees in electrical and computer engineering from the University of British Columbia, Canada, in 2009 and 2012, respectively. He worked in the consulting division of PricewaterhouseCoopers from 2005 to 2007 and from 2010 to 2011. In 2012, he joined the Faculty of Indraprastha Institute of Information Technology, New Delhi.

Amarjeet Singh received the B.Tech. degree in electrical engineering from IIT Delhi in 2002, and the M.S. and Ph.D. degrees in electrical engineering from the University of California at Los Angeles, USA, in 2007 and 2009, respectively. He was a Research and Development Electrical Engineer for Tejas Networks, Bengaluru, India, for two years. He acceded to the Faculty of the Indraprastha Institute of Information Technology, New Delhi, in 2010, with a joint appointment in Electronics and Computer Science Department.